JOURNAL OF VIROLOGY, Feb. 2002, p. 1309–1327 Vol. 76, No. 3
0022-538X/02/$04.00+0 DOI: 10.1128/JVI.76.3.1309–1327.2002

Relative Neurotropism of a Recombinant Rhabdovirus Expressing a Green Fluorescent Envelope Glycoprotein

Anthony N. van den Pol,[1]* Kevin P. Dalton,[2] and John K. Rose[2]

Departments of Neurosurgery[1] and Pathology,[2] Yale University School of Medicine, New Haven, Connecticut 06520

Received 6 August 2001/Accepted 29 October 2001

A new recombinant vesicular stomatitis virus (rVSV) that expresses green fluorescent protein (GFP) on the cytoplasmic domain of the VSV glycoprotein (G protein) was used in the mouse as a model for studying brain infections by a member of the *Mononegavirales* order that can cause permanent changes in behavior. After nasal administration, virus moved down the olfactory nerve, first to periglomerular cells, then past the mitral cell layer to granule cells, and finally to the subventricular zone. Eight days postinoculation, rVSV was eliminated from the olfactory bulb. Little sign of infection could be found outside the olfactory system, suggesting that anterograde or retrograde axonal transport of rVSV was an unlikely mechanism for movement of rVSV out of the bulb. When administered intracerebrally by microinjection, rVSV spread rapidly within the brain, with strong infection at the site of injection and at some specific periventricular regions of the brain, including the dorsal raphe, locus coeruleus, and midline thalamus; the ventricular system may play a key role in rapid rVSV dispersion within the brain. Thus, the lack of VSV movement out of the olfactory system was not due to the absence of potential for infections in other brain regions. In cultures of both mouse and human central nervous system (CNS) cells, rVSV inoculations resulted in productive infection, expression of the G-GFP fusion protein in the dendritic and somatic plasma membrane, and death of all neurons and glia, as detected by ethidium homodimer nuclear staining. Although considered a neurotropic virus, rVSV also infected heart, skin, and kidney cells in dispersed cultures. rVSV showed a preference for immature neurons in vitro, as shown by enhanced viral infection in developing hippocampal cultures and in the outer granule cell layer in slices of developing cerebellum. Together, these data suggest a relative affinity of rVSV for some neuronal types in the CNS, adding to our understanding of the long-lasting changes in rodent behavior found after transient VSV infection.

The *Mononegavirales* order of viruses includes the rhabdoviruses (rabies virus and vesicular stomatitis virus [VSV]), paramyxoviruses (mumps virus and measles virus), filoviruses (Marburg and Ebola viruses), and Borna disease virus. Many members of this order can invade the central nervous system (CNS) with neurological complications that may persist long after the virus is eliminated. Lack of in vivo models for such infections has hampered neurovirology studies in this field.

VSV has a very wide host range, from vertebrates, including humans, to insects, including sand flies, house flies, and mosquitoes, which may spread the virus among mammals (42). It is a natural pathogen in a wide range of animals, including livestock. Infected animals develop vesicles in the mouth, particularly on the tongue and also on the hooves and udders of mares and cows; VSV symptoms in livestock are similar to those seen with hoof and mouth disease, caused by a different virus. Animals produce a strong humoral and cellular immune response to VSV, and most animals quickly recover from the disease. VSV is distantly related to rabies virus; however, unlike rabies virus, VSV is highly cytopathic.

VSV is a bullet-shaped, enveloped virus and replicates and directs gene expression in the cytoplasm. Its genome is a single negative-sense, nonsegmented strand of RNA that contains only five genes encoding structural proteins (N, L, P, M, and G) and has a total size of 11.161 kb. The single envelope glycoprotein (G) is responsible for attachment of the virus to a cell surface receptor and fusion of the viral to endosomal membranes, allowing entry of the viral RNA into the cell (42).

Previous work has suggested that VSV is neurotropic. The virus can gain entry to the CNS from the outside environment by infecting the olfactory receptor neurons in the nasal passage (1, 18, 23, 25, 30). After intranasal inoculation, VSV can be found in the CNS, but little is found outside the brain (18, 30), as studied in mice and rats. If VSV disperses within the brain before it is eliminated by the immune system, it can result in permanent behavioral alterations, neurological complications, or death. Of considerable interest is the possibility the virus may show a selective affinity for some neuron types. For instance, VSV infections of the brain affect the locus coeruleus and dorsal raphe, two neuronal loci that synthesize norepinephrine and serotonin, respectively (18, 21). Animals that survive VSV infection show a permanent reduction in serotonin and also show permanent behavioral alterations, including hyperactivity and poor performance on the Morris water maze (21), which last long after the virus has been eliminated by the immune system. VSV infections of the CNS thus may provide an important model of transient viral infections of the brain leading to neurological or mental dysfunction.

In the present study, we used a recombinant VSV (rVSV) engineered to express a GFP reporter gene fused to the cytoplasmic domain of the VSV G protein that allows the active

* Corresponding author. Mailing address: Department of Neurosurgery, Yale University School of Medicine, 333 Cedar St., New Haven, CT 06520-8082. Phone: (203) 785-5823. Fax: (203) 737-2159. E-mail: anthony.vandenpol@yale.edu.

virus to be tracked in brain and in vitro. To clearly define cell preferences in vivo and in vitro, with a focus on neurons, and given the high mutation rate of the virus and the different strains of virus used in previous work from several different laboratories, we have examined both in vitro and in vivo conditions of rVSV infection with a single virus whose sequence is defined (7). One advantage of this recombinant virus is that live infected cells can be detected at an early stage (3 h) by the appearance of the G-GFP protein, and after 6 h, the morphology of the infected cells is defined in exquisite detail by GFP at the plasma membrane of the entire dendritic arbor.

MATERIALS AND METHODS

rVSV. The rVSV was made from reconstitution of the Indiana strain of VSV from DNA (15) coding for a positive-sense strand of RNA, as described in detail elsewhere (7). Briefly, the coding sequence for an enhanced redshifted and mammalian codon-corrected GFP (EGFP; Clontech) was fused to the coding sequence of the VSV G protein and incorporated as an extra gene downstream of the unmodified VSV gene. VSV particles contain about 1,200 molecules of the G protein on the viral surface (39). A recombinant virus that expresses GFP fused to the VSV G protein was generated from a combination of four plasmids that were cotransfected (29) into baby hamster kidney cells (BHK-21) to generate rVSV. vTF7–3, a recombinant vaccinia virus, was used to provide T7 RNA polymerase, an enzyme necessary for gene expression. rVSV from plates showing a cytopathic effect and GFP expression was titrated on BHK-21 cell monolayers, individual green plaques were isolated, and virus from them was grown on BHK-21 cells. This virus expresses both wild-type G and G-GFP fusion proteins, which form heterotrimers. The heterotrimers are transported to the cell surface and incorporated into budding virions.

Intracerebral and transnasal infection. Adult mice, 35 to 40 days old at the time of inoculation, were used for intracerebral injections ($n = 8$) and nasal application ($n = 9$). After anesthetizing the mouse with Nembutal (60 mg/kg of body weight), a small hole was made in the top of the skull. A Hamilton microsyringe was used to deliver a small volume (0.1 to 0.5 μl) of sterile buffer containing VSV (10^8 PFU/ml). The tip of the injection needle was lowered 3 mm down from the top of the skull, 1.5 mm lateral to right of the midline, and the VSV was administered by slow application of pressure. Four mice received injections aimed at the rostral part of the brain (striatal area), and four mice received injections aimed more caudally at the hippocampal area.

After the mice had been anesthetized with pentobarbital (Nembutal;60 mg/kg), 15 μl of sterile medium containing VSV was applied to each of the external nares, resulting in infection of the nasal cavity. At 2 ($n = 2$), 5 ($n = 2$), or 8 days ($n = 5$) postinoculation (p.i.), mice were given an overdose of anesthetic (Nembutal; 100 mg/kg) and perfused transcardially with physiological saline followed by freshly prepared 4% paraformaldehyde. Serial sections with a thickness of 10 to 20 μm were cut on a freezing sledge microtome through the entire brain. From the serial sections, 1 of every 20 sections was mounted in a cryoprotectant buffer on glass slides, giving a representative view of the entire brain. After a coverslip was added, sections were saved in a freezer until studied.

Primary mouse brain culture. Embryonic brain tissue was used for primary neuronal culture. Cells were plated on glass coverslips that had been pretreated with polylysine to enhance the affinity of cells to the substrate. In some experiments, we used cultures of whole brain, and in others, we used selective cultures of single brain regions, often the hippocampus. More details of the culture methodology can be found elsewhere (41). In some experiments, we used cultures of various organs to compare relative VSV infection and production. Animal use in these experiments was approved by the University Committee on Animal Use.

Human primary culture. Tissue from human cerebral cortex was used for primary culture. Tissue was removed solely for medical reasons and for the patient's benefit. Tissue was from brain tumors that included both part of the tumor and tissue at the edge of the tumor. Use of the tissue after surgical removal was approved by the Human Investigations Committee of the University.

Live brain slices. After animals were given an overdose of Nembutal, brains were removed and cut into 200-μm-thick slices. Slices were maintained at the gas-fluid interface on a Millipore membrane at 37°C with 5% CO_2. Brain slices were fed with Neurobasal (Gibco/BRL). Slices were infected with rVSV by placing a drop of virus-containing medium on the slice (10^6 PFU per slice).

Ultrastructural analysis. To study the fine structure of VSV in infected cells, mouse hippocampal cultures were used after 7 days in vitro. Six to 8 h p.i., cultures were fixed with 3% glutaraldehyde in a 0.1 M cacodylate buffer for 1 h, washed with the same buffer, postfixed in1% osmium tetroxide, dehydrated through an ascending ethanol series that included uranyl acetate in the 70% ethanol, and then treated with propylene oxide and embedded in Epon. The glass substrate was removed with liquid nitrogen, and ultrathin sections were cut and stained with uranyl acetate and lead citrate. Photomicrographs were taken on a Phillips or JEOL electron microscope.

Microscopy. Most photomicrographs from cultures or slices were taken of live cells. Micrographs of tissue sections were made from fixed brain material. Nikon or Olympus IX70 or SZX12 microscopes with xenon or mercury illumination were used to examine infected material. A variety of excitation and emission filters (Chroma, Brattleboro, Vt.) were used to detect the GFP-G fusion protein and ethidium homodimer. Differential interference contrast (DIC) or phase-contrast images were also used to examine fields of cells for control purposes to give an idea of the relative number of cells showing expression of the viral reporter gene. A Spot or RT digital camera (Diagnostic Imaging, Ann Arbor, Mich.) interfaced with a Macintosh computer was used. Contrast and saturation were corrected digitally with Photoshop. Images were printed on an Epson 870 or 900 printer or a Kodak 8650 printer. When several micrographs on a single plate are shown to compare levels of infection, identical parameters of image acquisition and processing were used.

RESULTS

By using a recombinant virus that expresses GFP attached to its G protein, we examined rVSV infection of cells from mouse and human CNS. Previous work with VSV has been done in vitro and in vivo, but often by different laboratories with different strains of VSV leading to varying results. Because VSV has a high rate of mutation (1 in 10,000 nucleotides, or 1/virion), different VSV strains may vary considerably in their nucleotide and amino acid sequences, particularly in the G protein that mediates virus attachment and fusion to host cells. Previous work has suggested that VSV is nonselective in its target cell (42), or that, in the brain, it may be very selective for subsets of neurons (30). To study viral entrance and infection of the brain, we first examined mouse brains after intranasal inoculations and compared these results with those from brains infected intracerebrally or from brain slices infected with VSV. To further examine VSV cellular tropism, we next studied VSV infections of mouse and human cells in culture and then compared VSV infections in developing and mature neurons in vitro. These studies are important both to characterize this recombinant VSV, which has not previously been used to study brain cells, and to study virus dispersal and infection in the CNS.

Intranasal inoculation. A number of viruses, including those in the mononegavirales family such as rabies (14) and Borna disease virus (34), can enter and infect the brain through the nasal path. VSV may gain access to the brain through the olfactory nerve (17, 25, 30). To verify this with the recombinant virus used in the present study, we administered VSV (10,000 PFU) into each of the external nares. By 2 days p.i., GFP expression could be found in the olfactory nerves within the olfactory bulb (Fig. 1A). Green fluorescence was found in some, but not all, regions of the olfactory nerve, including the olfactory axons that terminated in the glomeruli of the olfactory bulb (Fig. 1C and D). In regions of the bulb in which the GFP-expressing olfactory nerves terminated, GFP-expressing periglomerular cells were found (Fig. 1B to D). Strong expression of green fluorescence was found in the presynaptic dendrites of the periglomerular cells, particularly on the plasma

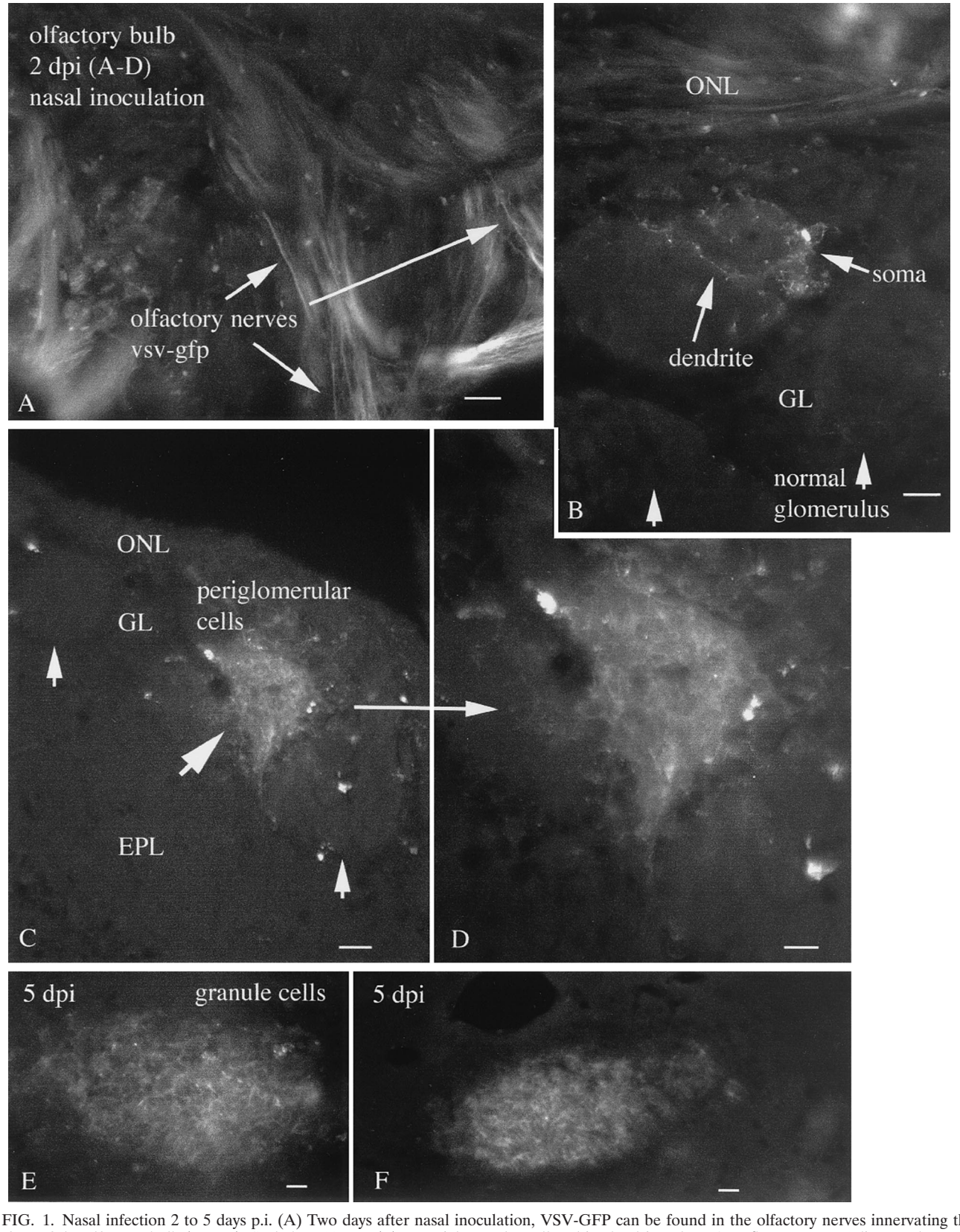

FIG. 1. Nasal infection 2 to 5 days p.i. (A) Two days after nasal inoculation, VSV-GFP can be found in the olfactory nerves innervating the surface of the olfactory bulb (arrows). Scale bar, 30 μm. (B) A periglomerular cell and its dendrites show GFP fluorescence. Adjacent glomeruli show no sign of infection. Scale bar, 25 μm. (C) A single glomerulus shows strong infection, with many cells expressing GFP. Adjacent glomeruli show only a small amount of infection in one or two cells. Scale bar, 25 μm. (D) Higher magnification of panel C showing dense packing of infected periglomerular cells. Scale bar, 12 μm. (E) Near the center of the bulb, a high level of infection is found. Scale bar, 15 μm. (F) More caudally, a group of cells near the subventricular zone are infected. Scale bar, 15 μm. ONL, olfactory nerve layer; GL, glomerular layer; EPL, external plexiform layer.

membrane at the cell surface (Fig. 1B). Infection of the glomerular layer was quite heterogeneous. Some glomeruli were full of infected green fluorescent neurons (Fig. 1C and D), whereas others showed few infected cells (Fig. 1B). In mice treated with VSV nasally, both left and right olfactory bulbs showed similar levels of VSV infections. Many glomeruli showed no signs of VSV infection.

By 5 days p.i., many of the cells in some glomeruli showed signs of cell death. Cells showed fragmentation and lost the smooth GFP expression at the cell surface, and GFP product became granular as infected cells degenerated. GFP expression in the periglomerular layer was attenuated. As at the shorter time interval of 2 days p.i., many glomeruli showed no signs of infection and no sign of cell death. As suggested by immunostaining for VSV antigens (12), VSV G-GFP expression was attenuated in the mitral cells compared with the strong expression in the glomerular and granule cell regions of the bulb. Clusters of granule cells showed expression of GFP. Also infected was a region of granule cells near the center of the bulb and the rostral extension of the ventricle, as well as caudally along this cell group (Fig. 1E and F). The two cell types that show the strongest levels of VSV infection, the periglomerular and granule cells, are both interneurons that in most cases use γ-aminobutyric acid (GABA) as their inhibitory neurotransmitter (35).

Interestingly, at 8 days after nasal inoculation, little fluorescence indicative of viral infection of live cells was detectable in the olfactory bulbs or the brains, suggesting a considerable depression in VSV infection in the olfactory bulb (Fig. 2A and B). That the lack of active infection was not the result of inadequate inoculation a priori was indicated by several factors. A pathway of dead cell debris could be found in the olfactory bulb and in the rostral brain. At this stage, no evidence for live infected cells was detected, and no GFP remained in the olfactory bulb in five of five brains. However, GFP-labeled debris from recently dead cells could be found as far caudal as the region just medial to the rostral nucleus accumbens in the area of the subventricular zone in four of five brains (Fig. 2C to E). This region is a source of neuronal precursor cells that migrate into the olfactory bulb, even in the adult, and give rise to interneurons within the bulb (16, 19).

In contrast to the four mice that showed no sign of active infection 8 days p.i., one mouse brain showed strong infection in the preoptic area restricted to one side of the third ventricle (Fig. 3A and B). This was highlighted by strong GFP fluorescence in many cells here and by a region in the ventral preoptic area where GFP expression had been lost, but degenerating cells were found that had a granular appearance and showed a dull red fluorescence, a by-product of the degeneration of cells infected with the GFP-expressing virus (Fig. 3C). No GFP, no cellular degeneration, and no red fluorescence were found on the contralateral side of this brain, either in the neuropil or in the cell bodies (Fig. 3). Little GFP was found in the ependymal cells on the side of the preoptic area contralateral to the infected side of the brain. Despite the neuronal death in these nasally infected mice, they appeared healthy and showed no obvious signs of poor health. Control experiments ($n = 4$) were also done with nasal administration of a GFP-expressing recombinant mouse cytomegalovirus (CMV) (41) in adult mice, using the same number of PFU as used for VSV. No infection by CMV was found in the mouse olfactory bulb 2 to 4 days p.i. These data indicate that viral movement into the brain through the olfactory path is a unique port of entry for some viruses, but not others.

Thus, with one exception, VSV dispersal appeared to be limited to regions of the olfactory system, particularly with a direct relationship to the olfactory bulb. No obvious signs of retrograde transport of VSV to cells of the brain that send fibers into the bulb were found in these studies: these negative areas include the olfactory cortex, the diagonal band, locus coeruleus, and raphe. Similarly, little evidence of anterograde transport and release of the virus in those regions of the brain that receive direct axonal input from the mitral cells was found. Areas that receive afferent input from the projection neurons of the bulb include the piriform cortex, olfactory tubercle, and entorhinal cortex (35); none of these areas showed signs of infection in the present study. Similarly, no infection was found in the lateral olfactory tract, the pathway by which mitral and tufted cells project caudally to the brain. These data suggest that although VSV may move in the olfactory nerve from the mucosa to the olfactory bulb, this transport may not generalize to retrograde or anterograde axonal transport in all neurons related to the olfactory system. Because the cells in the different laminae of the bulb communicate by dendrodendritic synapses, axonal transport would not be required for transcellular movement of the virus within the bulb. Instead, VSV could move between synaptically coupled dendrites or between adjacent cells to move from the bulb periphery into the center of the bulb. This would be consistent with our ultrastructural analysis that revealed VSV budding from both perikarya and dendrites, as well as uptake by both perikarya and dendrites.

Intracranial inoculation. In the preceding section, we found that dispersal of VSV after intranasal inoculation was limited primarily to the olfactory system. This could be due to an immune response that reduced virus spread or to a lack of viral affinity (including attachment, uptake, protein synthesis, and replication) for neurons outside the immediate olfactory system, or it could be due to local interferon responses. To test the hypothesis that rVSV can infect a broad spectrum of cells in the brain not restricted to olfactory neurons, we used a microsyringe to deliver 0.5 μl of VSV (10^8 PFU/ml) directly into the brain ($n = 8$), thereby bypassing the olfactory system. Two days p.i., mice appeared to be in poorer health and showed less evidence of grooming and less activity. Infection was detected both at the site of injection and at sites a considerable distance from the injection site. All mice receiving direct intracerebral injections showed GFP expression at the injection site and in other regions of the brain. Cells with a neuronal morphology were found in the cerebral cortex, striatum, thalamus, substantia nigra (Fig. 4A and B), hypothalamus (Fig. 4C), hippocampus (Fig. 4D), thalamus (Fig. 4E,F), hindbrain, and other regions. Some cells showed punctate labeling within the cell body and dendrites (Fig. 4E and F), suggestive of an early stage of VSV infection, as correlated with time-lapse analysis of VSV infections in culture (described below). Other cells showed strong labeling of the plasma membrane of the soma and dendrites, correlating with later stages of infection. In addition, particularly at the site of infection, GFP-labeled cellular debris could be found indicative of cellular degeneration after infection.

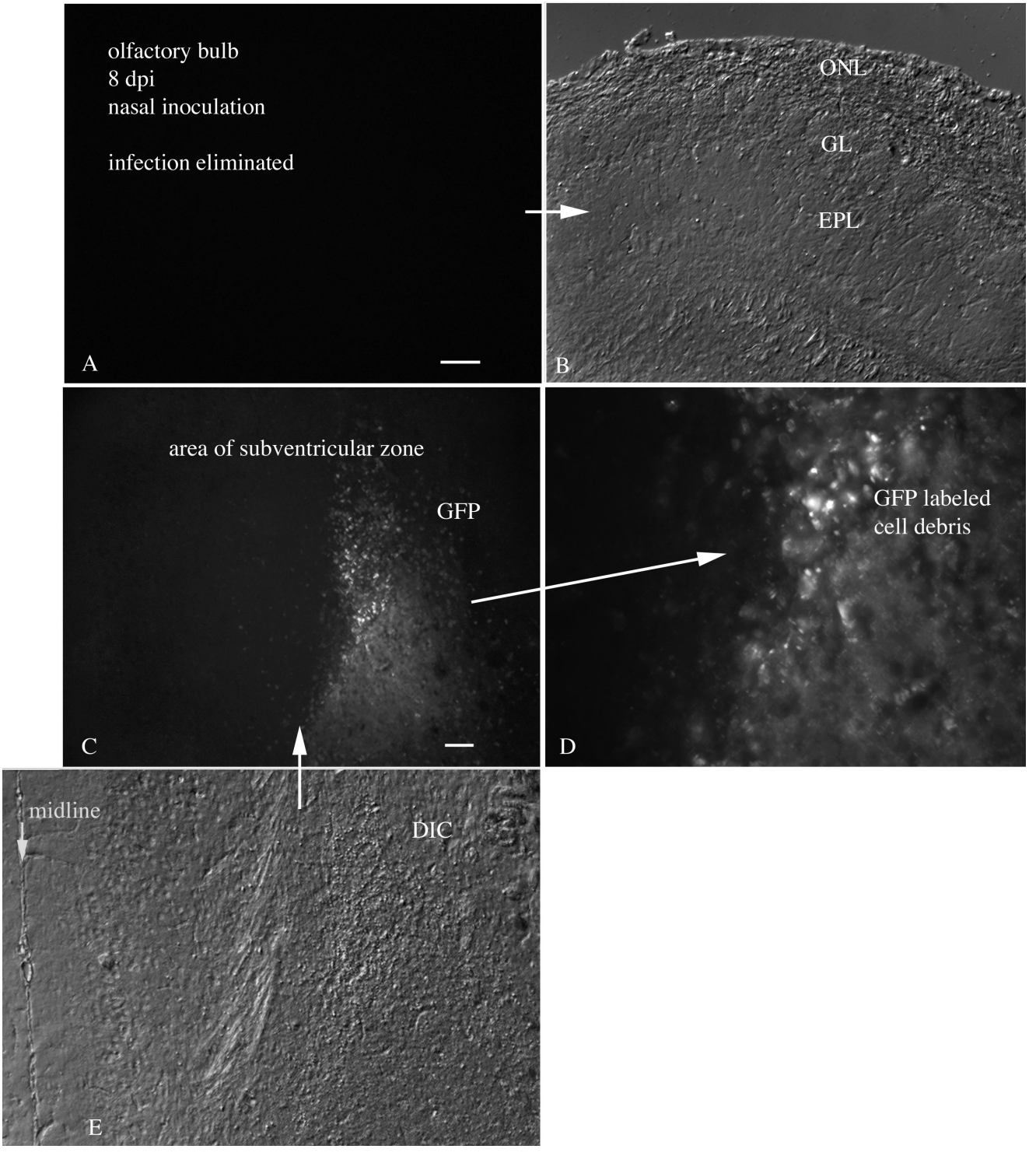

FIG. 2. Nasal infection 8 days p.i. (A) Eight days after infection, no trace of GFP remains in the olfactory bulb. (B) DIC image of the same section shown in panel A. (C) Caudal to the bulb, GFP-labeled cellular debris is found in the subventricular zone. Scale bar, 60 μm. (D) Higher magnification of panel C. (E) Aligned DIC image of the fluorescent section shown in panel C. The midline is on the left. ONL, olfactory nerve layer; GL, glomerular layer; EPL, external plexiform layer.

In mice in which the injection site was close to a ventricle, we noted that the virus diffused into the ventricular system, and from there to other ependymal cells lining the ventricles. VSV-infected neurons were found at a number of sites near the ventricles, in particular the locus coeruleus (Fig. 5A to C) and dorsal raphe. In these cases, the corresponding nuclei on both sides of the brain were infected. Although many other types of neurons were situated within the same distance from the ven-

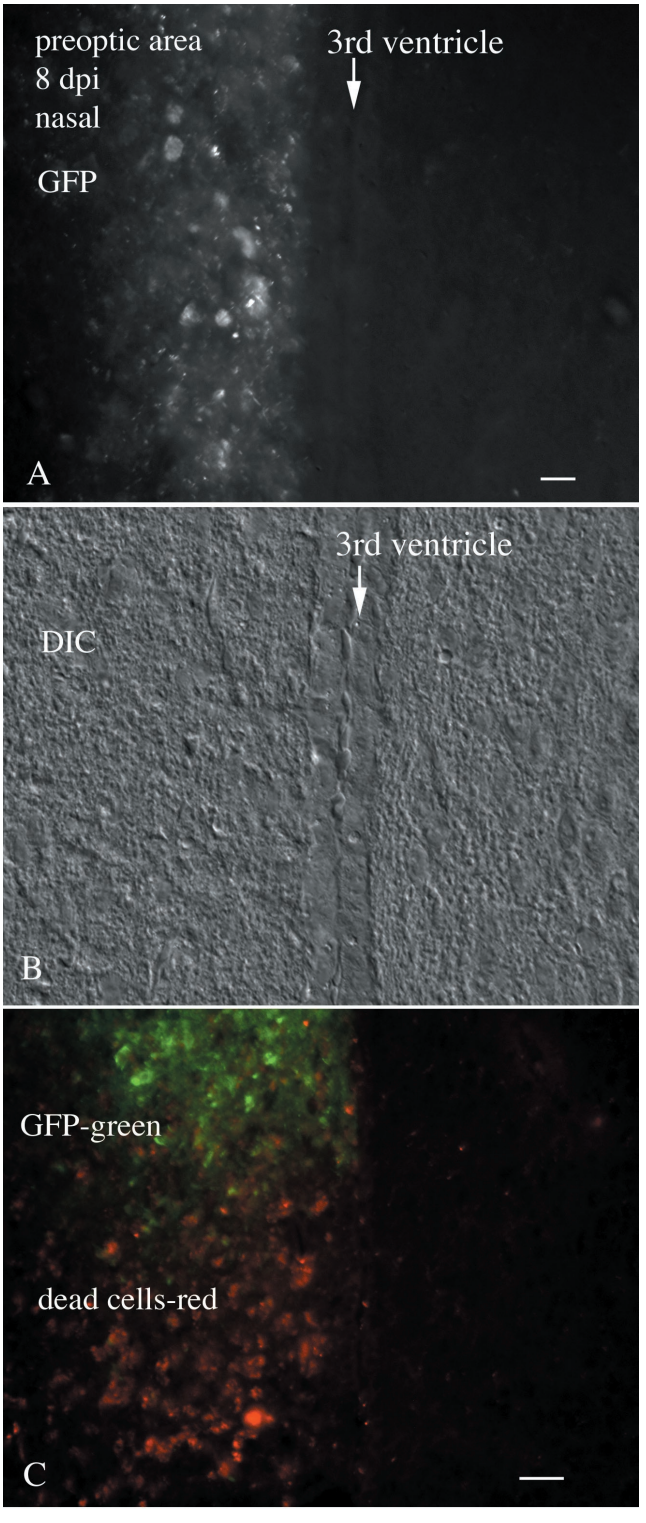

FIG. 3. Nasal infection-preoptic area infiltration. (A) Cellular debris showing GFP label of the preoptic area in the single animal showing viral dispersion outside the olfactory system. Only the left side of the brain shows VSV infection of the preoptic area. In this section, no infection of the ependymal cells that line the ventricle is detected. (B) DIC image of the same field shown in panel A. (C) In a caudoventral direction in the preoptic area, GFP-labeled cells are seen at the top of the micrograph, and reddish cells indicative of degenerated cells are seen more ventrally. Scale bar, 30 μm.

tricular surface (for instance, the granule cells of the cerebellum), strong levels of VSV infection of these cells were not detected (Fig. 5A to C). In some mice, small injections were made, and the virus did not diffuse into the ventricle. For instance, when VSV administration was confined to the hippocampus (Fig. 5D), no infection of the ventricular lining was found. In mice showing no infection of the ventricular lining, no infection was found in the dorsal raphe or in the locus coeruleus (Fig. 5E and F), despite the fact that both regions send axonal projections to the hippocampus. Parallel data exist for transnasal infections of the olfactory bulb, which also receives direct axonal projections from the raphe and locus coeruleus, but these areas also showed no sign of viral infection from 2 to 8 days p.i. We found no direct evidence for retrograde axonal transport of VSV and in fact found a lack of viral infection in brain regions that send axons to the infected olfactory bulb. It is possible that retrograde axonal transport may contribute to viral dissemination under some conditions. However, our data do support the hypothesis that VSV movement through the cerebrospinal fluid may play an important role in dissemination.

Rapid infection and expression of transgene. To examine the time course and cellular distribution of VSV infections and transgene expression, we studied CNS cultures at 60-min intervals after inoculation. One remarkable aspect of VSV infection is the very rapid expression of VSV G-GFP after viral inoculation. At 1 h p.i. with 10^6 PFU per culture, no GFP expression was found. Similarly, in cells not inoculated with VSV, green fluorescence typical of GFP was not found at any time. By 3 h p.i., the Golgi apparatus of infected neurons had already turned bright green (Fig. 6C to E). During the next 1 to 2 h, small green vesicles containing VSV G-GFP were transported out of the Golgi apparatus and into the somatic cytoplasm and proximal dendrites (Fig. 6F and G), and the plasma membrane began turning green. By 6 to 8 h p.i., the plasma membrane of the entire dendritic arbor and neuron cell body was fluorescent. From a morphological perspective, the expression of GFP in the plasma membrane revealed the dendritic structure in striking detail and could be found in proximal and distal dendrites, in dendritic spines, and, in young cells, in dendritic growth cones (Fig. 7). The detail of the neuronal surface was clearer with incorporation of the VSV G-GFP in the plasmalemma than was apparent with other recombinant viruses, such as CMV, that generated GFP expression in neuronal cytoplasm (41). VSV G-GFP fluorescence was minimal in long, fine processes of constant diameter, a morphology typical of axons, consistent with previous suggestions of selective transport of VSV G protein to dendrites (9, 10). Most (98%+) cells in culture showed GFP expression at later stages of infection.

The relative time of expression of VSV G-GFP in different regions of the cell (i.e., Golgi, dendritic membrane vesicles, and plasma membrane) was dependent on the titer of inoculated virus. With low levels of virus (10^4 PFU; multiplicity of infection [MOI] <1), the time taken to reach a particular state might be 6 h longer. Neurons showed early signs of infection. Cells with a typical astrocyte morphology, characterized by a flat, sheet-like morphology with neurons growing on top, were also infected by VSV; these cells showed a lower level of VSV G-GFP fluorescence, and fluorescence appeared later than

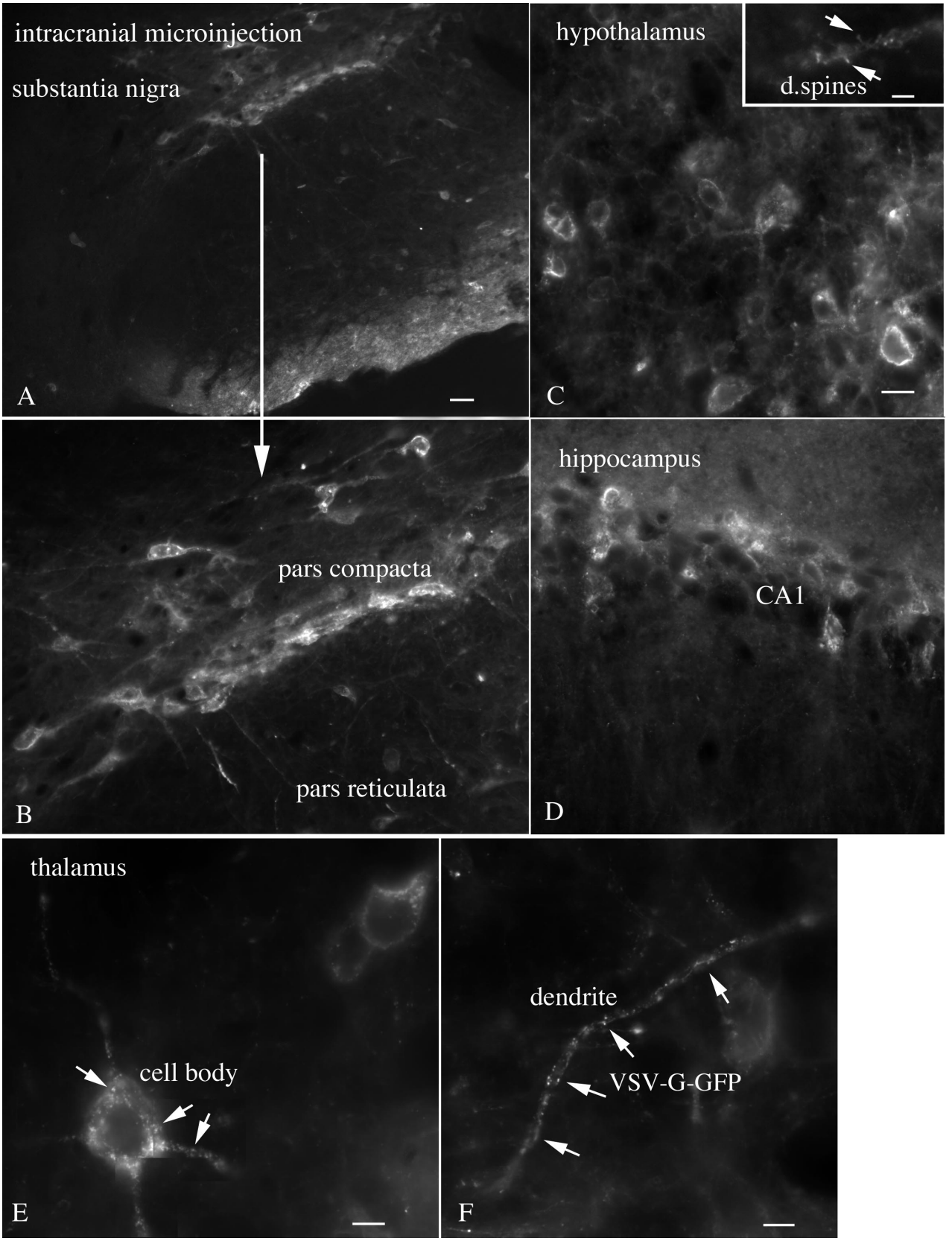

FIG. 4. Intracranial administration of VSV. Widespread infection, including substantia nigra, hypothalamus, hippocampus, and thalamus, is shown. (A) Two days after intracranial injection of VSV, cells of the pars compacta are infected with VSV. A few cells in the pars reticulata are also infected. Scale bar, 40 μm. (B) Higher magnification of the infected cells of the substantia nigra. Neurons of the medial hypothalamus (C; scale bar, 13 μm), hippocampus (D; scale bar, 20 μm), and thalamus (E and F) are infected with VSV. An inset in panel C shows dendritic spines (arrrows). (E and F) Granule appearance of VSV G-GFP in the cell body and dendrites of thalamic neurons indicative of an early stage of infection. (E) Scale bar, 6 μm. (F) Scale bar, 5 μm.

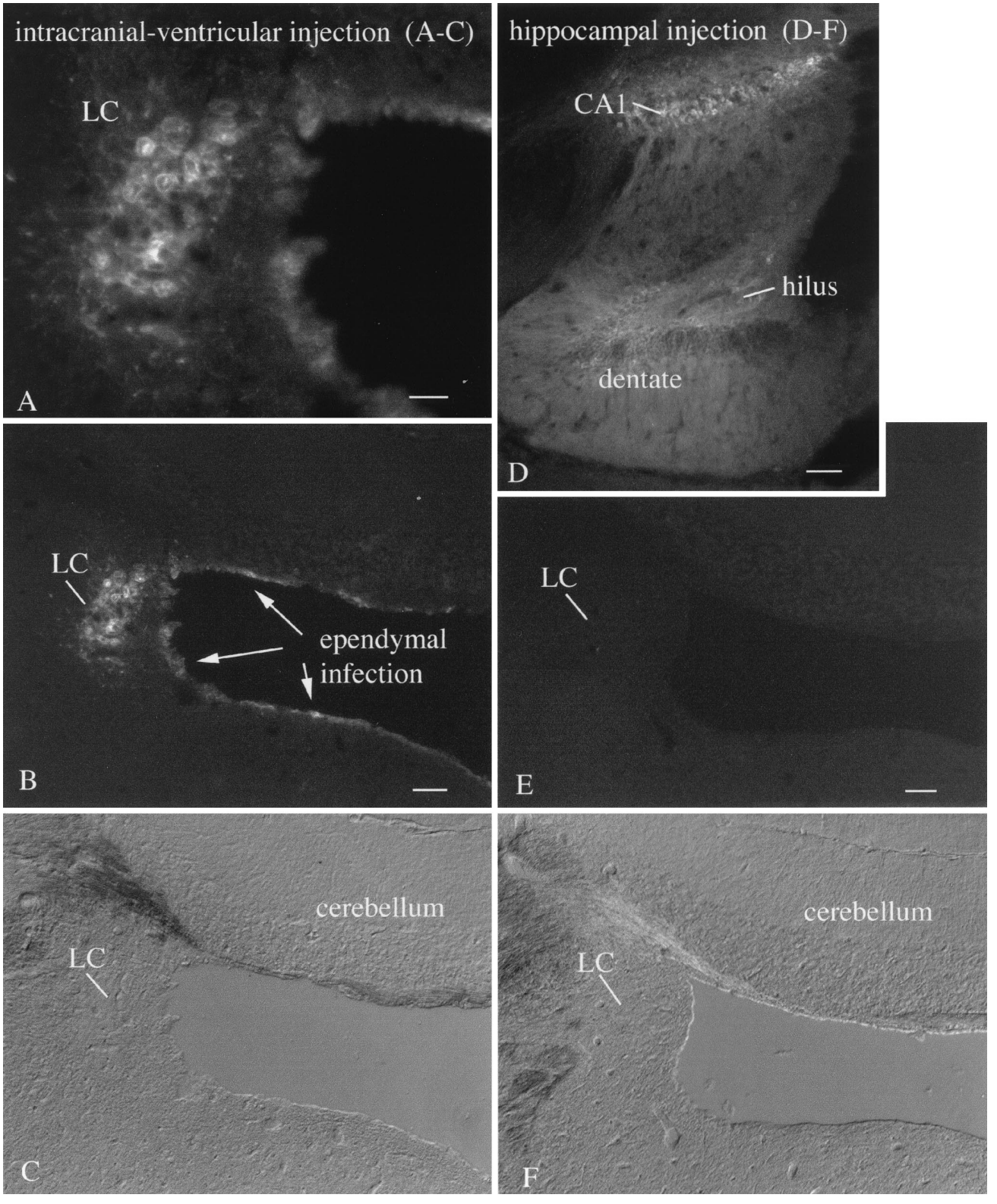

FIG. 5. Locus coeruleus (LC) selective neurotropism. (A) After intracerebral injections of VSV into rostral brain regions where VSV was found in the ependymal cells of the ventricular system, the LC showed a high level of infection. Scale bar, 40 μm. (B) A lower magnification shows the same field, with infection of the nearby GFP-expressing ependymal cells. Other neurons also adjacent to the ventricular system show only relatively low levels of infection. The LC was infected bilaterally, but only the left LC is shown here. Scale bar, 125 μm. (C) DIC micrograph of the same area shown in panel B. (D) A small injection into the hippocampus shows infection of CA1 and the dentate gyrus and hilus. On other sections, not shown here, part of CA3 was also infected. Scale bar, 225 μm. (E) In the absence of VSV in the ventricular system, no infection of the LC is detected. Scale bar, 125 μm. (F) DIC micrograph of the same field shown in panel E.

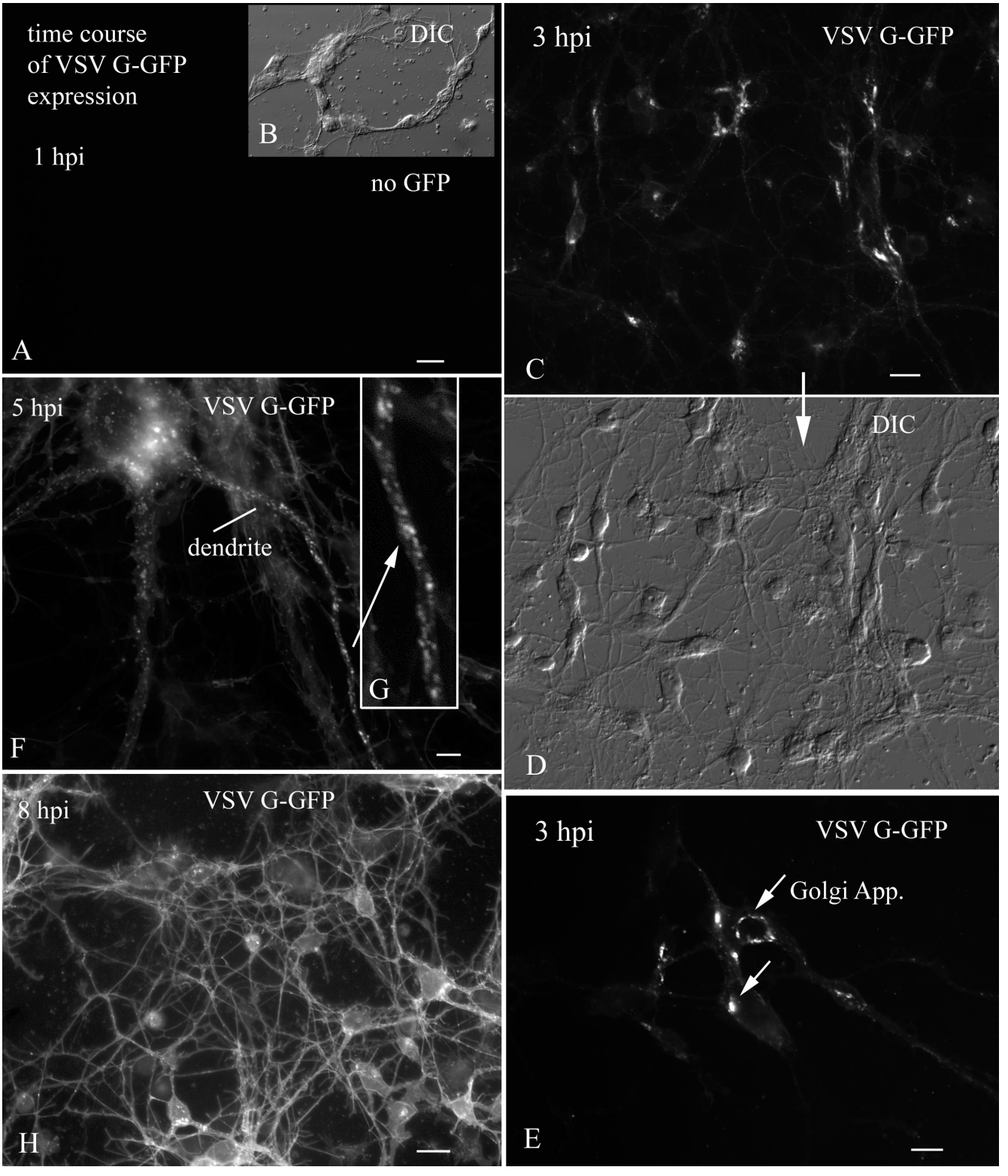

FIG. 6. Time course of VSV G-GFP expression after inoculation. (A) By 1 h p.i., no GFP reporter expression was detected. Scale bar, 20 μm. (B) The same field as in panel A, but with DIC. (C) At 3 h p.i., VSV G-GFP expression begins to show in the Golgi apparatus. Scale bar, 25 μm. (D) DIC image of the same field shown above in panel C. (E) High magnification of the neurons in which the primary organelle expressing GFP is the Golgi apparatus. Scale bar, 10 μm. (F) At 5 h p.i., large numbers of large vesicles containing VSV G-GFP are found in the dendrites. Scale bar, 3 μm. (G) Higher magnification of the dendrite indicated by an arrow in panel F. (H) At 8 h p.i., strong expression of VSV G-GFP is found on dendritic and somatic membranes. Scale bar, 25 μm.

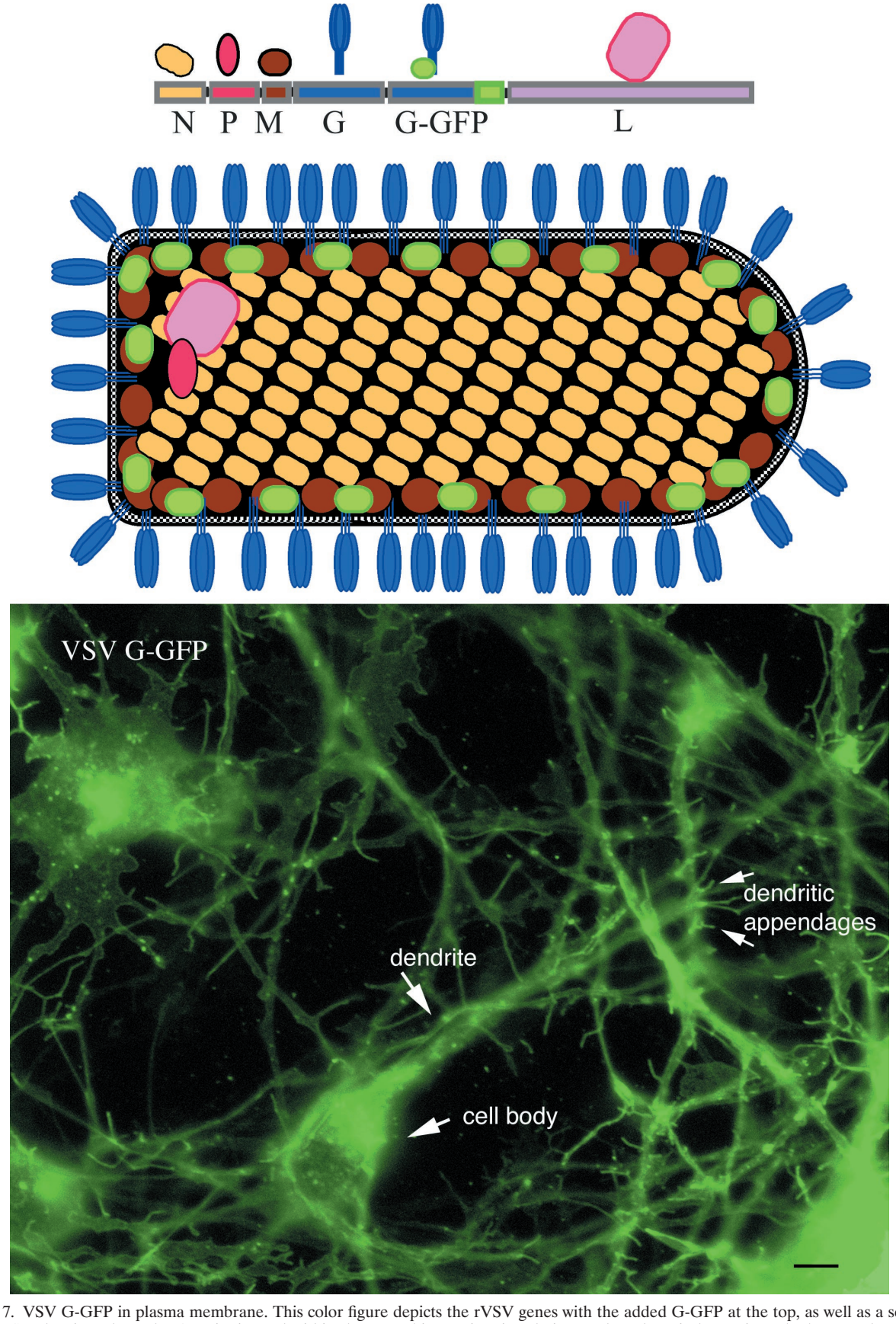

FIG. 7. VSV G-GFP in plasma membrane. This color figure depicts the rVSV genes with the added G-GFP at the top, as well as a schematic of the rVSV showing where the GFP is situated within the recombinant virus in relation to the other viral proteins. The bottom shows a CNS culture after 2 days in vitro and infected 6 h prior to imaging. At this stage of infection, heterogeneity of expression of rVSV G-GFP is found among different cells. With time, the fluorescence of all cells will increase further. Bar, 6 μm.

that seen in cells with a neuronal morphology. Although some previous reports based on immunocytochemistry had suggested the VSV G immunoreactive protein was patchy (9), the VSV G-GFP showed a smooth expression throughout the plasma membrane on both glial cells and neurons. Patchy expression of GFP was seen only during early stages of infection when GFP-labeled large vesicles were transported in the dendritic cytoplasm, visualized by time-lapse video microscopy, or when cells began to degenerate (see below). An advantage of the rVSV used in the present paper is that it allows easy detection of infected cells within a short time after infection and while the infected cells are still living. The rapid and robust signal generated by the rVSV in culture suggest that it is less likely that CNS cells were infected but not detected after intranasal inoculation, as described above.

CNS cultures compared with other cell types. VSV has been called a neurotropic virus (30). This was initially based on experiments with intranasal and intracerebral injections, followed by a bioassay based on the response of test mice to intracerebral injections of tissue homogenate and the suggestion that the virus selectively targeted CNS cells, with relatively little infection of other types of cells. We compared mouse CNS cultures with cultures of heart, skin, bone, and kidney, and with a hamster cell line, BHK-21, used to grow the virus. Cultures of all cell types showed robust infections, as demonstrated by GFP expression in infected cells 8 h p.i. (Fig. 8A to F) The BHK-21 cell line showed the highest level of GFP expression, and skin cells showed the lowest. Figure 8A and F show representative examples of infections in these cultures, with the GFP expression on the left and the corresponding DIC micrograph of the same area on the right. From these data, we calculated the relative percentage of neurons showing VSV infection, as indicated by the GFP expression in the infected cell (Fig. 9). In sister cultures, 1 h after inoculation, the medium was washed three times and then maintained overnight. The next day, the infected cells were harvested and tested for virus proliferation by using a standard plaque assay. In general, the level of GFP fluorescence correlated with virus production, with BHK-21 cells showing the highest level of productive infection and skin cells showing the lowest level. Brain cells were similar to bone, heart, and kidney cells with respect to GFP fluorescence and virus replication (Fig. 9). Thus, in culture, no preference for cells of the CNS was detected relative to heterogeneous mixtures of cells from other organs. These data suggest that, in vitro, VSV does not demonstrate any preference for CNS cultures over non-CNS cells, but does show a productive infection of CNS after inoculation.

VSV affinity for young CNS cultures. In the course of examining VSV inoculations of cultures of different in vitro ages, GFP expression was detected sooner and was stronger in young cultures than in old cultures. Hippocampal cultures of cells 6 and 21 days in vitro (DIV) were compared. As shown in Fig. 10, the young cultures showed strong GFP fluorescence 6 h p.i. (5×10^5 cells, done in triplicate), whereas only a low level of fluorescence was seen in the older cultures. Similar differences were found at 12 h p.i. This difference is interesting in that previous reports have suggested that older mice are more resistant to VSV infections in the brain than younger mice (30). These culture data suggest that some of the developmental sensitivity to VSV infections may be due to some intrinsic resistance in older CNS cells. This would be independent of the maturation of the immune system, often considered to be the primary factor attenuating viral infections of the adult CNS.

Ultrastructural examination of rVSV budding. Electron microscopy was used to examine rVSV-infected mouse CNS cultures derived from P1 hippocampus, and maintained in vitro for 7 days prior to inoculation. Because cultures had been washed several times after inoculation, viral particles found outside cells were probably progeny virus from infected cells. Cultures fixed 6 to 8 h after inoculation showed signs of viral replication and budding. Viral particles were found between cultured cells: the shape of the VSV at the ultrastructural level was similar to that reported for the wild-type virus, with a bullet-shaped structure, one short end rounded, and the other flat; some particles had the shape of a cucumber, with both ends being slightly rounded (Fig. 11A). Virus particles budded from neurons with the round end of the virus pointing out from the plasma membrane initially, followed by the blunt end (Fig. 11B). VSV budding from the plasma membrane was found both in perikarya and in dendrites. Signs of viral endosomal uptake in both cell bodies and dendrites were also found. At this stage of infection, although VSV was already replicating in host cells, the infected cells show a fairly normal morphology without obvious signs of degeneration or death that would overtake the culture in the succeeding few hours. We found no obvious signs of VSV uptake or release from processes that were determined to be axons based on clusters of synaptic vesicles and synaptic membrane specializations, based on 15 electron micrographs.

VSV causes cell death in human and mouse CNS cultures. CNS cultures ($n = 60$) were used to study VSV infections in vitro. Cells from each area, including hypothalamus, hippocampus, olfactory bulb, cortex, spinal cord, and whole brain, showed high levels of infection and G-GFP expression. With an MOI of 5 or greater, VSV was cytopathic for all cells from all regions of the mouse brain. The cytopathic effect of VSV was confirmed with ethidium homodimer (Molecular Probes), a stain that reveals dead cells by their red nuclear fluorescence (Fig. 12). In early stages of infection, neurons that were infected with VSV had a normal morphology. However, within 10 to 15 h, neurons showed substantial signs of degeneration. By 20 h p.i. (MOI = 10), GFP labeling progressed from the continuous label on the cell membrane to a more punctate staining indicative of neuronal degeneration (Fig. 12A). Almost all cells in culture showed GFP fluorescence indicative of VSV infection and later showed a breakdown in the plasma membrane and nuclear membrane, indicated by red nuclear staining with ethidium homodimer that labels dead cells (Fig. 12A to C). In addition, as cells degenerated, they often lost their adhesion to the substrate and floated up into the medium.

Pieces of human cortex removed in the course of surgical treatment for brain tumors were dispersed in monolayer cultures. Most of the cells in these cultures had the morphology of glial cells, with a small number of cells showing neuronal morphology with long processes arising from the cell body. Within 22 h of VSV infection (MOI = 10), all inoculated cultured cells expressed the GFP viral transgene (Fig. 13A and D). Red staining with ethidium homodimer revealed that all cells from inoculated cultures appeared to be dead or dying (Fig. 13B and

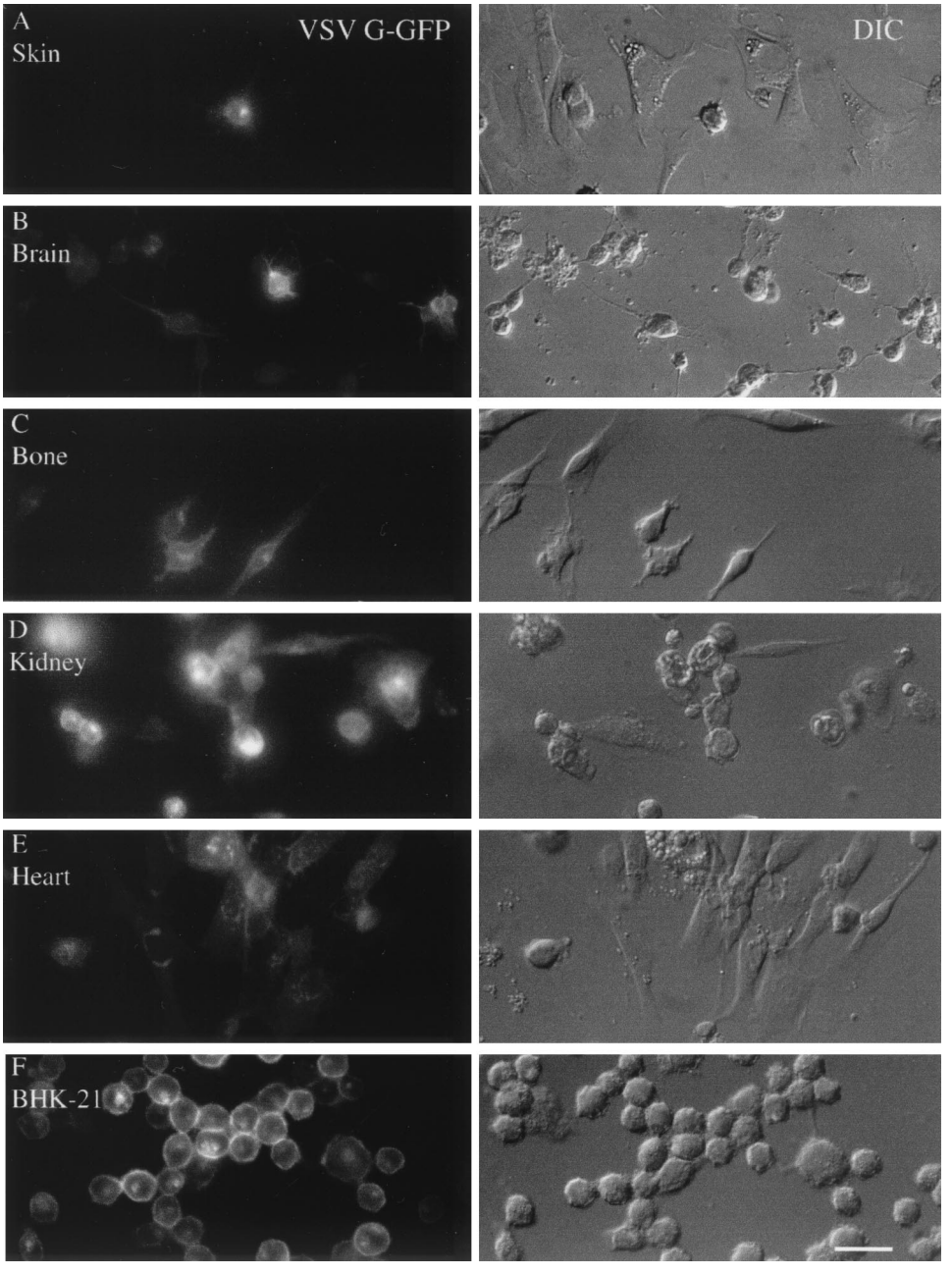

FIG. 8. Multiple cell types are infected by VSV. Primary cultures were made from skin (A), brain (B), bone (C), kidney (D), and heart (E). (F) BHK-21 cells that are used to propagate the virus were used for the purpose of comparison. Cultures were fixed with paraformaldehyde 8 h p.i. The expression of VSV G-GFP is shown on the left, and the same microscope field is shown on the right side with DIC. Scale bar, 30 μm.

C). Sister cultures of noninfected control human CNS cells remained healthy and showed no green fluorescence and almost no staining with ethidium homodimer: less than 2% of the control cells showed red labeling (Fig. 13E and F). These data indicate that in the absence of an intact immune system, VSV produces a cytopathic infection in all cultured human CNS cells. A good percentage of the cells in the human CNS cultures may be abnormal, given that the source was from the area of a tumor. Previous reports have suggested that VSV may have an affinity for rapidly dividing cells typically found in tumors (2, 38) and may have potential as an oncolytic virus.

Mouse brain slice infection cell preference. Infection of subsets of neurons within the brain could be dictated in part by the ability of the virus to have access to a particular set of cells. Inoculation of living brain slices in vitro allows direct rVSV access to cells in the mouse slice. Thick brain slices (200 μm) were maintained on a suspended membrane, and VSV was applied to the surface of the slice. Infected cells were found in slices from all areas studied, including hippocampus, cerebral and cerebellar cortex, and hypothalamus.

Cerebellar granule cells go through their final cell division around postnatal days 6 to 9. After mitosis in the external

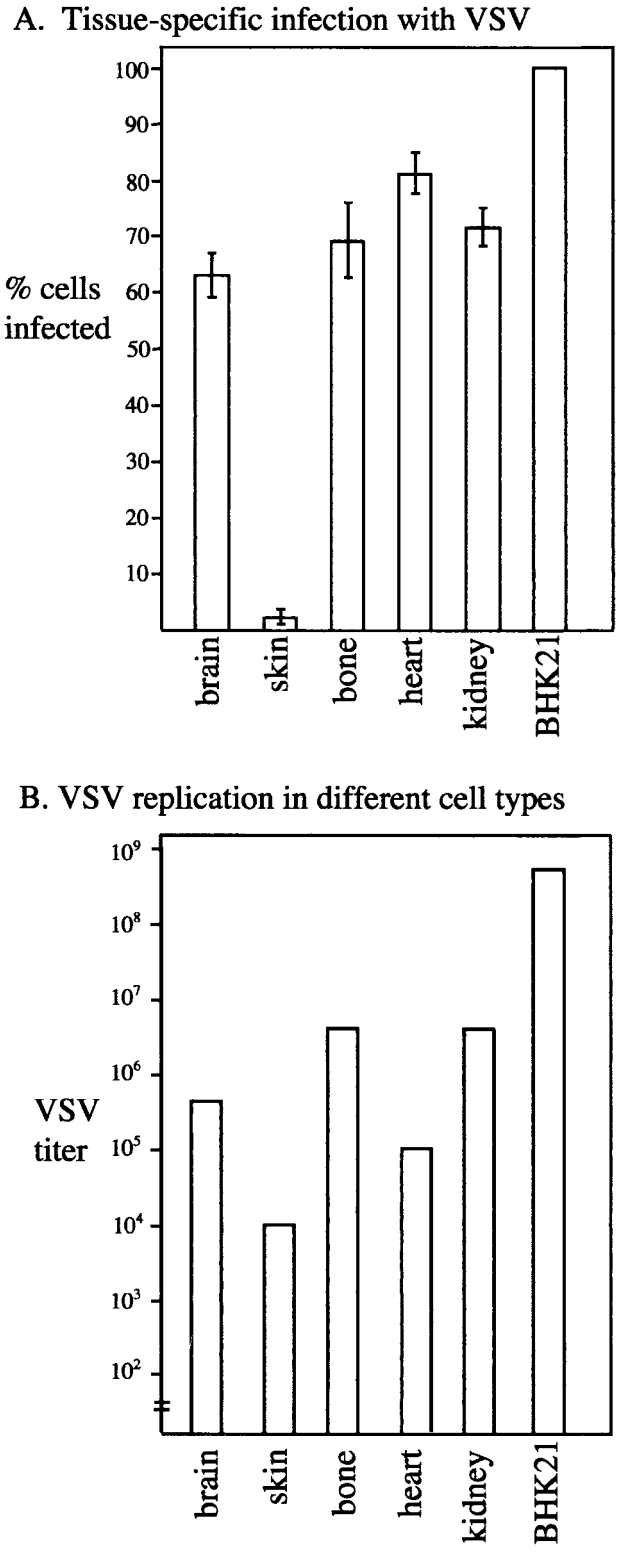

FIG. 9. Bar graphs showing number of infected cells and VSV replication. (A) Tissue-specific infection with VSV. Based on the VSV infections shown in the preceding micrographs, the relative number of GFP cells (fluorescence) and total cells (DIC) was determined in eight microscope fields. Means and standard errors of the mean are shown in the top bar graph. (B) VSV replication in different cell types. To determine the rate of replication in the different cells, sister cultures were harvested (three cultures per cell type), and the viral titer was determined by incubating the culture medium with BHK-21 cells and determining the virus concentration by plaque assay. The mean level of viral replication is shown here.

granule cell layer, they migrate down through the Purkinje cell layer and settle in the internal granule cell layer. Thus, in a single postnatal section, one can compare the relative levels of infection of VSV for cells undergoing mitosis compared with the same class of cells after completion of their migration and during the outgrowth of the dendritic processes. Both internal and external granule cell layers showed green fluorescence, indicative of VSV infection (Fig. 14). In seven of eight cerebellar slices, the external granule cell layer showed a greater level of fluorescence (Fig. 14), suggesting a higher level of VSV infection. Granule cells in the outer granule cell layer had no dendrites, and strongly fluorescent neurons appeared tightly packed together. Cell bodies and the short dendrites of the granule cell neurons in the internal granule cell layer showed a less intense level of virally mediated fluorescence. As a control, we also tested a recombinant mouse CMV, a member of the herpesvirus family, that contains a GFP coding sequence (41) in sister slices of the same brains. CMV showed relatively less infection of the cerebellar granule cells, but did infect some of the large cells in the Purkinje cell layer. These experiments show that VSV may show relative cell preferences in brain slices in vitro and may have an affinity for some developing neurons even in the absence of an intact immune system.

DISCUSSION

The severity of CNS damage caused by a neurotropic virus can be viewed as a race between virus dispersal and immune system detection and response to curb the infection. A virus that spreads quickly may do a greater degree of damage than one that spreads slowly. VSV infection is rapid. We show here that within 3 h of neuronal infection, the VSV G protein is already synthesized and transported to the Golgi apparatus, and by 4 h postinfection, viral proteins have been transported to the dendritic and somatic plasma membrane. Within 6 h of neuronal infection, progeny viruses begin budding off from the infected cell. Yet despite the rapid rate of VSV infection and replication, the mouse brain still restricts the VSV to an olfactory compartment after nasal inoculation.

rVSV G protein appears to be transported anterogradely to the terminal ends of olfactory nerves in the olfactory bulb, a critical requirement for budding of infectious VSV from the nerve ending. The virus spreads from the olfactory nerve centrally, through the periglomerular and granule cells, and then centrally in the bulb to the ventricular zone. Release of VSV by the cell body and dendrites may account for local spread of the virus. Of relevance to this is the fact that the periglomerular, mitral, and granule cells are connected by dendrodendritic synapses (35), and as ultrastructurally verified with the rVSV, new virus buds from, and is taken into, dendrites and somata. Axons are not required for much of the intercellular communication within the bulb, and therefore may not be involved in VSV transcellular movement between the synaptically connected cells. In most cases, the recombinant virus did not escape from the olfactory system; neither anterograde nor ret-

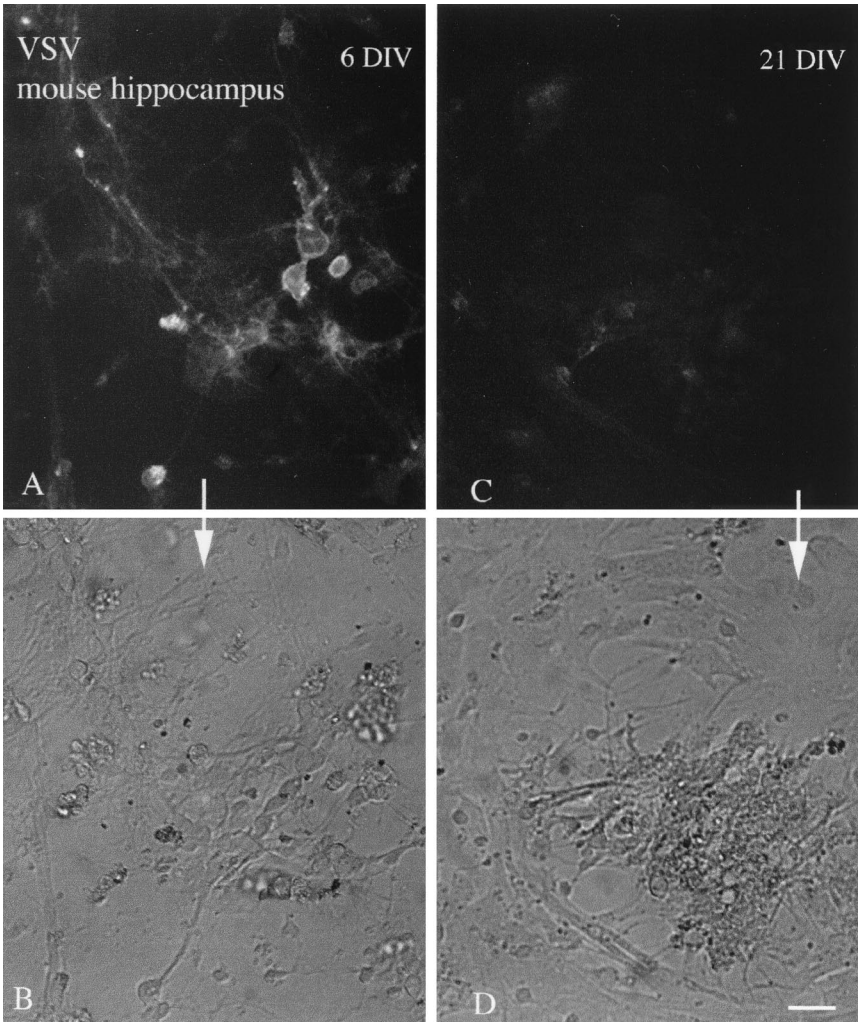

FIG. 10. Immature cultures show enhanced VSV infection. Hippocampal cultures after 6 or 21 days in vitro (DIV) were infected with VSV (10^6 PFU), and photomicrographs were taken at 6 h p.i. (A) A number of cells show infection indicated by the GFP fluorescence in 6 DIV cultures. (B) The same field as in panel A, shown with phase contrast. (C) Only a low level of infection was found in older cultures 21 DIV. (D) Phase-contrast image of the same field shown in panel C. Scale bar, 45 μm.

rograde axonal transport led to infection outside the bulb, and in most mice, the virus was eliminated from the bulb 8 days p.i. VSV entry into the brain is more likely via a nasal route than after intravascular administration, and the virus is more likely to target the olfactory system over the trigeminal system as a port of entry into the brain (25).

Transient VSV infections in the brains of immature mice and rats may cause permanent changes in behavior, perhaps from loss of raphe serotonin or locus coeruleus norepinephrine neurons (1, 18, 21). After intracerebral administration, infection of the locus coeruleus and dorsal raphe occurred only when evidence of viral infection of the adjacent ventricular lining was present. The raphe and locus coeruleus send strong axonal projections to the bulb and hippocampus. However, when local infection of bulb or hippocampus was generated experimentally and no evidence of VSV was detected in the ventricles, then no infection was found in either the locus coeruleus or dorsal raphe, findings inconsistent with retrograde axonal transport of VSV in these systems. Thus, these data favor a conservative interpretation that the rVSV used here has an intrinsic affinity for neurons of these brain regions and reaches them by dispersal through the CSF. Our data do not preclude anterograde or retrograde axonal transport as an additional mechanism of movement of VSV within the CNS, but suggest it may not be the primary mode of dispersal to some regions for which the virus has an affinity and which may play a key role in the behavioral disturbances found long after viral infection is eliminated. Analysis of published immunocytochemical micrographs from other work (12) suggesting retrograde VSV transport shows consistent infection of the ventricular system adjacent to the infected neurons.

The developing brain is more susceptible to VSV infections than the adult brain (18). Although this developmental difference is generally attributed to the maturation of the immune system, our finding of a VSV preference in vitro, with no immune system, for developing hippocampal neurons and newly divided premigratory cerebellar granule neurons suggests that VSV may also have an intrinsic affinity for developing neurons. VSV cell selectivity was also demonstrated by Lundh et al. (17), who showed a selective infection of olfactory

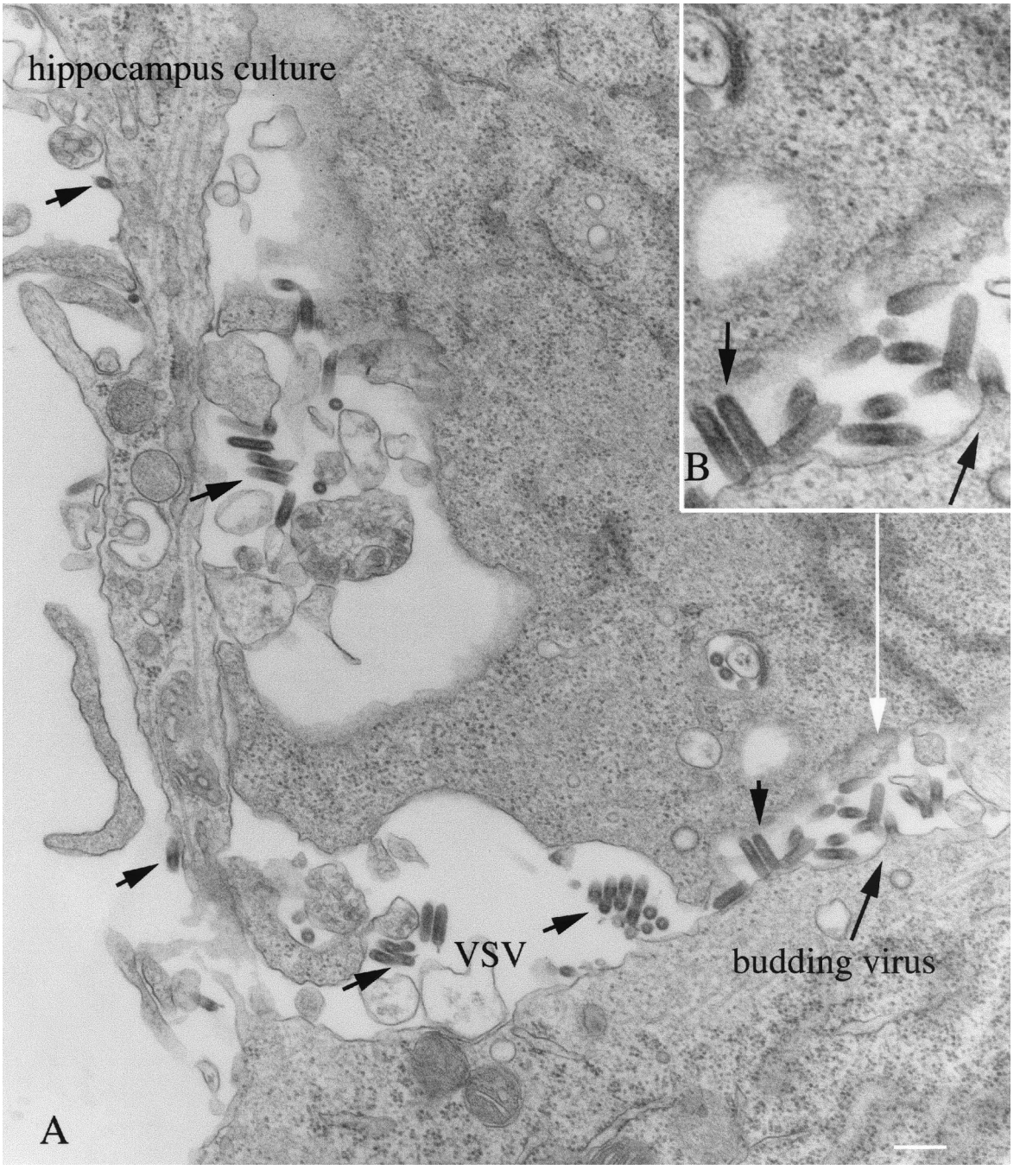

FIG. 11. Ultrastructure of infected cultures. Hippocampal neurons were infected with VSV and fixed 8 h later. VSV can be found in the extracellular space between cells and budding from the cell body (long black arrow). VSV particles are elongated, with a bullet-shaped morphology. The ultrastructure of infected cells at this stage appears relatively normal.

receptor neurons with little infection of respiratory cells with VSV application to the nose, in contrast to control experiments with Sendai virus that showed the opposite cell preference. In parallel, we found no infection of the olfactory bulb after nasal inoculation of CMV, confirming the selectivity of this pathway for VSV. Selective infection of the brain was found after VSV nasal administration, with little infection of other peripheral organs (30).

Different strains of herpes simplex virus (43) or pseudorabies virus (4) may have affinities for different neuronal phenotypes. The same may be true for different strains or mutants of VSV (6, 8). Previous work has suggested a permanent reduction in serotonin (20, 21) after VSV infection. We found a direct infection of these cells with the rVSV used in the present study, indicating that the loss of serotonin neurons is not an indirect consequence of viral infection (e.g., is not due to loss of axonal target or trophic factors needed for survival), but rather is due to a cytopathic effect of direct and selective viral

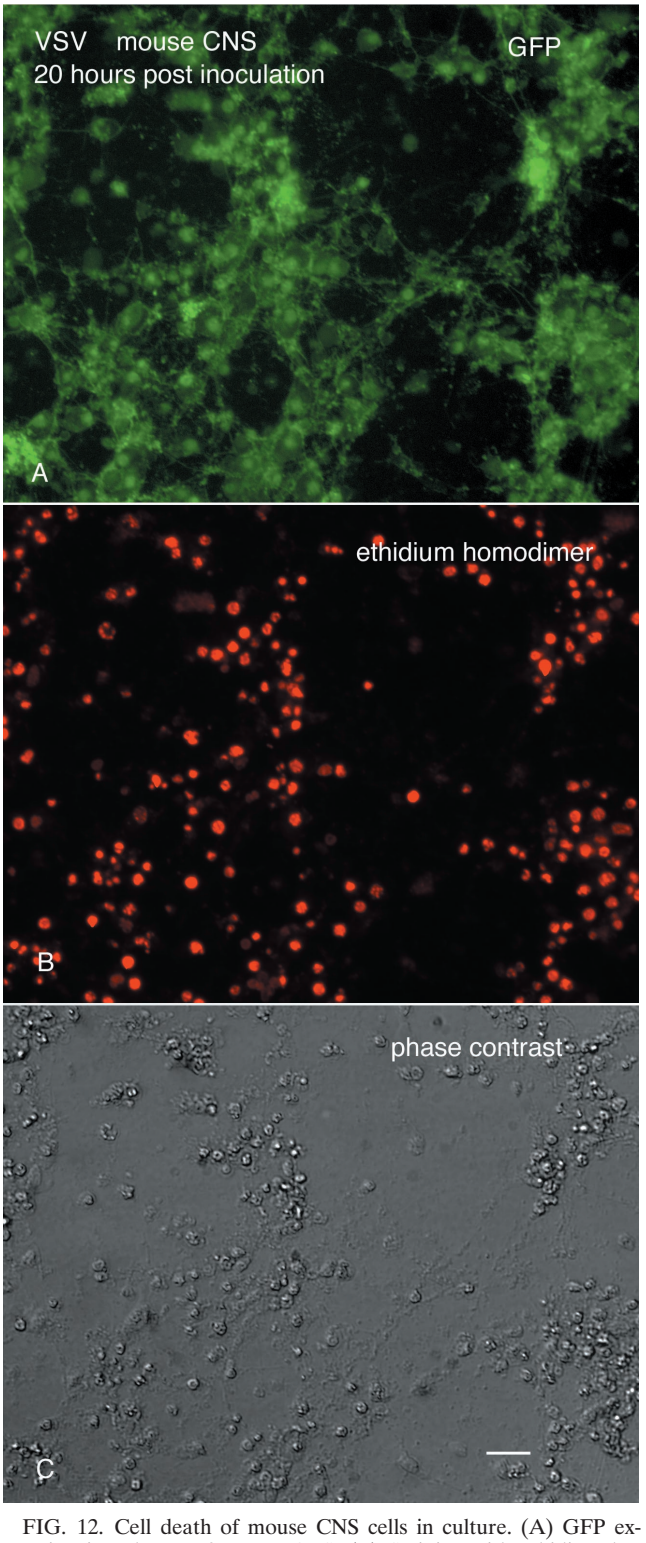

FIG. 12. Cell death of mouse CNS cells in culture. (A) GFP expression in cultures of mouse CNS. (B) Staining with ethidium homodimer reveals that most of the cells shown in panels A and C are dead. (C) Phase-contrast image of the same field, showing degenerated cells. Scale bar, 50 μm.

infection, and that the rVSV has similar cellular affinities to wild-type virus. In contrast to the restricted spread of rVSV within the CNS described here, more widespread CNS infections after intranasal administration have also been reported (11, 18, 25). Factors that may play a role in the spread of VSV within the CNS include age, gender, virus strain, mouse strain, species, and viral titer (18, 25). In addition, rVSVs derived from DNA (e.g., G protein fused with GFP [this study] or with influenza virus hemagglutinin) are less pathogenic in mice than wild-type VSV (27).

Having shown that the recombinant VSV has a similar affinity for brain regions previously demonstrated for the wild-type virus and a preference for developing neurons, an unanswered question remains—why does the virus show an affinity for these cells? It could be due to a number of factors. One possibility is that the virus has a preferential affinity for a viral receptor on the surface of these cells. If so, the affinity would not be absolute, because we find that virtually all cells in vitro are infected by the virus. Previous work has suggested the viral receptor is not a protein, is present on a wide variety of cells, and may be phosphatidylserine (31). VSV is very promiscuous in which cells it infects in dispersed cells in vitro, as demonstrated by the infections of different cells from the mouse heart, skin, kidney, and bone in the present paper and from the wide dispersal of this virus across an unusually wide spectrum of host species, including most mammals, sand flies, house flies, and mosquitoes. Differences could also exist in cellular factors required for viral replication, assembly, transcription, or budding from the plasma membrane. The reason that nasal VSV infections stop within the olfactory system is probably not due simply to the cellular or humoral immune response generated by the virus, because when intracerebral injections of the virus are made at the time the virus is being eliminated from the olfactory system, a lethal response is found (30). Although cellular and humoral immunity may control VSV infections in the periphery, interferon may play an important role in the CNS (13, 22, 37, 40). That the cells of the olfactory system may use interferon or related antiviral molecules to reduce spread of VSV into the rest of the brain merits further exploration.

Other members of the *Mononegavirales* order can infect CNS cells and lead to neurological deficits. Some can be quite dangerous in the laboratory and require high levels of biosafety containment (Marburg and Ebola viruses), whereas others, such as measles virus, only infect primates, making some laboratory work difficult or impractical. Rabies, which can also lead to CNS infection after intranasal inoculation (14), is highly neurotropic and replicates in many mammals, but it is also deadly. VSV thus has substantial utility as a model for studying viral invasions of the CNS. We show that VSV produces a cytopathic and productive infection of all cultured mouse and human CNS cells. Although not considered a serious health hazard to humans, VSV infections may cause fever, weakness, nausea, and vomiting and are more prevalent in tropical than temperate climates. Rare cases of VSV-mediated encephalitis have been reported (24, 28). Both mouse and human immune systems are particularly responsive to VSV, and outside the brain, efficiently eliminate it within 7 days of infection. Recombinant VSV may be useful as a robust antigen delivery system for generating high-titer immune responses to

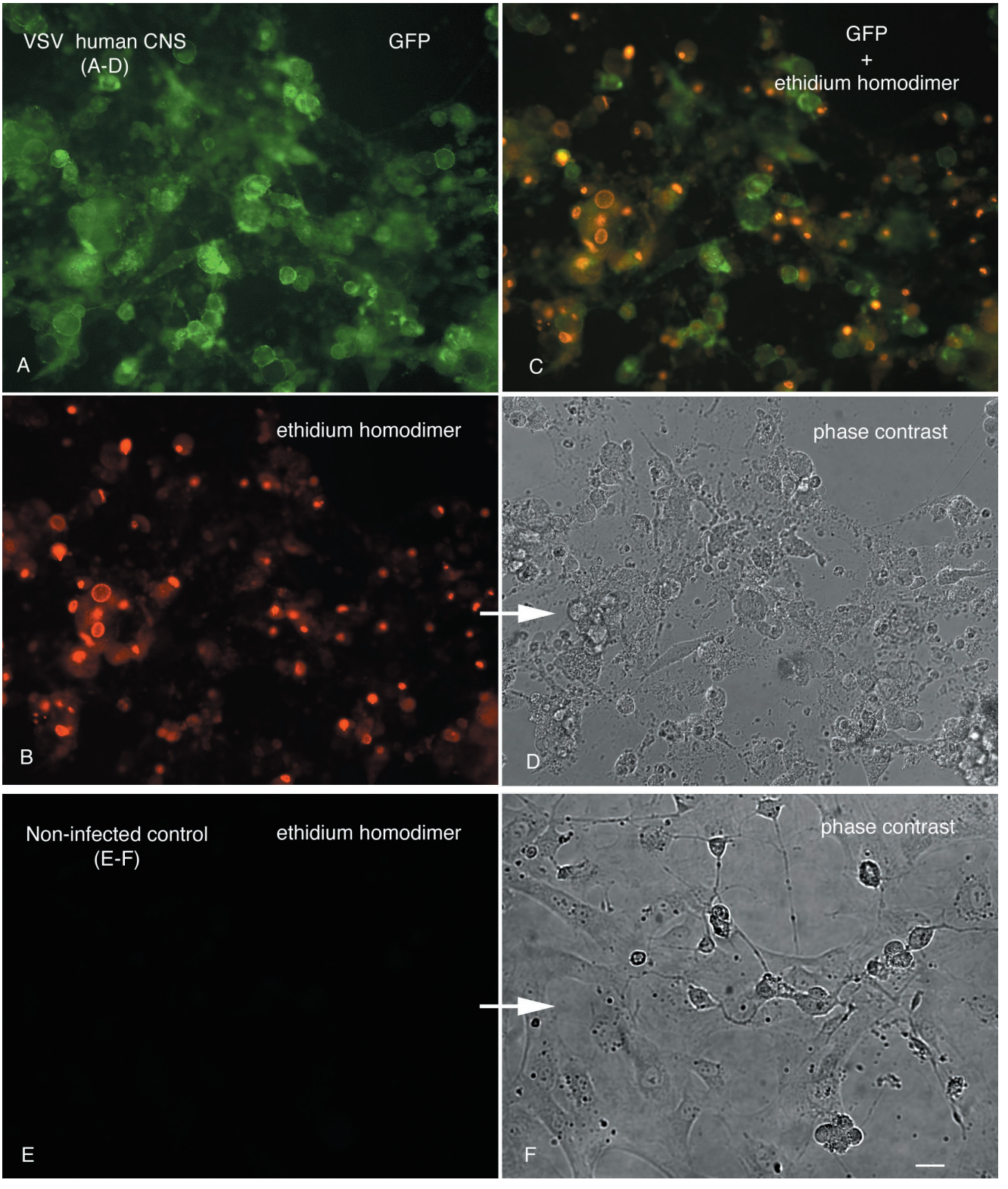

FIG. 13. VSV infection of human CNS cells in culture. Panels A to D show the same microscope field, but with different types of photic excitation. (A) VSV G-GFP. (B) Ethidium homodimer stains dead cells red. (C) Combination of GFP and ethidium homodimer. Overlap of GFP green and ethidium homodimer gives an orange coloration. (D) Phase-contrast image showing cellular debris after infection. (E and F) Normal noninfected control cultures. No GFP and no ethidium homodimer staining is seen in this field, shown in phase contrast in panel F. Scale bar, 35 μm.

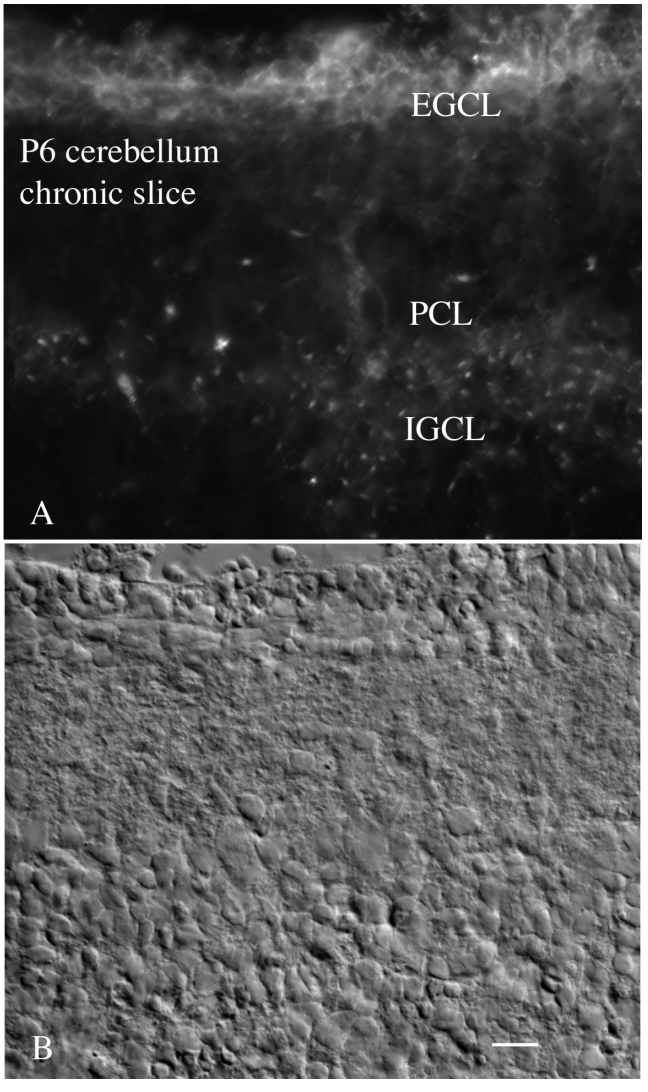

FIG. 14. Enhanced infection in younger neurons in cerebellar slice. (A) Postnatal day 6 thick slices were infected with VSV (10^5 PFU/slice). Many cells of the developing cerebellum were infected, but the highest level of infection is found in the external granule cell layer (EGCL), a region of dividing granule cell neurons. A lower level of infection is also found in the internal granule cell layer (IGCL) and in a few cells of the Purkinje cell layer (PCL). Scale bar, 35 μm.

other viruses, including HIV, respiratory syncytial virus, and influenza virus, based on recombinant VSV that contains genes from the other viruses fused to the gene coding for VSV G protein (3, 26, 32, 33).

rVSV infection of the mouse brain is a useful model for studying the neurological and behavioral consequences of transient CNS infections by neurotropic viruses. VSV shows a relative preference for developing neurons and for some neuronal types in the mature brain, and it may be axonally transported in some (olfactory nerve) but not other axon types. Although not the primary focus of our paper, the rVSV-GFP may prove to be a good candidate vector for selective labeling of some neurons for morphological studies. Infection results in a strong labeling of the plasma membrane of the entire dendritic arbor, including dendritic spines and growth cones. Other nonrelated viruses, particularly alpha herpesviruses, have proved invaluable as neuroanatomical tools (4, 5, 36).

ACKNOWLEDGMENTS

We thank Y. Yang and J. Santarelli for technical help and J. Piepmeier for tissue.

Research support was provided by NIH grants NS 10174, NS 34887, NS 31573, and AI 24345 and the National Science Foundation.

REFERENCES

1. **Andersson, T., A. K. Mohammed, B. G. Henriksson, C. Wickman, E. Norrby, M. Schultzberg, and K. Kristensson.** 1993. Immunohistochemical and behaviour pharmacological analysis of rats inoculated intranasally with vesicular stomatitis virus. J. Chem. Neuroanat. **6:**7–18.
2. **Balachandran, S., and G. N. Barber.** 2000. Vesicular stomatitis virus (VSV) therapy of tumors. IUBMB Life **50:**135–138.
3. **Boritz, E., J. Gerlach, J. E. Johnson, and J. K. Rose.** 1999. Replication-competent rhabdoviruses with human immunodeficiency virus type 1 coats and green fluorescent protein: entry by a pH-independent pathway. J. Virol. **73:**6937–6945.
4. **Card, J. P., P. Levitt, and L. W. Enquist.** 1998. Different patterns of neuronal infection after intracerebral injection of two strains of pseudorabies virus. J. Virol. **72:**4434–4441.
5. **Card, J. P., M. E. Whealy, A. K. Robbins, R. Y. Moore, and L. W. Enquist.** 1991. Two alpha-herpesvirus strains are transported differentially in the rodent visual system. Neuron **6:**957–969.
6. **Dal Canto, M. C., and S. G. Rabinowitz.** 1981. Murine central nervous system infection by a viral temperature-sensitive mutant: a subacute disease leading to demyelination. Am. J. Pathol. **102:**412–426.
7. **Dalton, K. P., and J. K. Rose.** 2001. Vesicular stomatitis virus glycoprotein containing the entire green fluorescent protein on its cytoplasmic domain is incorporated efficiently into virus particles. Virology **279:**414–421.
8. **Dille, B. J., J. V. Hughes, T. C. Johnson, S. G. Rabinowitz, and M. C. Dal Canto.** 1981. Cytopathic effects in mouse neuroblastoma cells during a non-permissive infection with a mutant of vesicular stomatitis virus. J. Gen. Virol. **55:**343–354.
9. **Dotti, C. G., J. Kartenbeck, and K. Simons.** 1993. Polarized distribution of the viral glycoproteins of vesicular stomatitis, fowl plague and Semliki Forest viruses in hippocampal neurons in culture: a light and electron microscopy study. Brain Res. **610:**141–147.
10. **Dotti, C. G., and K. Simons.** 1990. Polarized sorting of viral glycoproteins to the axon and dendrites of hippocampal neurons in culture. Cell **62:**63–72.
11. **Huneycutt, B. S., I. V. Plakhov, Z. Shusterman, S. M. Bartido, A. Huang, C. S. Reiss, and C. Aoki.** 1994. Distribution of vesicular stomatitis virus proteins in the brains of BALB/c mice following intranasal inoculation: an immunohistochemical analysis. Brain Res. **635:**81–95.
12. **Huneycutt, B. S., Z. Bi, C. J. Aoki, and C. S. Reiss.** 1993. Central neuropathogenesis of vesicular stomatitis virus infection of immunodeficient mice. J. Virol. **67:**6698–6706.
13. **Komatsu, T., Z. Bi, and C. S. Reiss.** 1996. Interferon-gamma induced type I nitric oxide synthase activity inhibits viral replication in neurons. J. Neuroimmunol. **68:**101–108.
14. **Lafay, F., P. Coulon, L. Astic, D. Saucier, D. Riche, A. Holley, and A. Flamand.** 1991. Spread of the CVS strain of rabies virus and of the avirulent mutant AvO1 along the olfactory pathways of the mouse after intranasal inoculation. Virology **183:**320–330.
15. **Lawson, N. D., E. A. Stillman, M. A. Whitt, and J. K. Rose.** 1995. Recombinant vesicular stomatitis viruses from DNA. Proc. Natl. Acad. Sci. USA **92:**4477–4481.
16. **Lois, C., and A. Alvarez-Buylla.** 1994. Long distance neuronal migration in the adult mammalian brain. Science **264:**1145–1148.
17. **Lundh, B., K. Kristensson, and E. Norrby.** 1987. Selective infections of olfactory and respiratory epithelium by vesicular stomatitis and Sendai viruses. Neuropathol. Appl. Neurobiol. **13:**111–122.
18. **Lundh, B., A. Love, K. Kristensson, and E. Norrby.** 1988. Non-lethal infection of aminergic reticular core neurons: age-dependent spread of ts mutant vesicular stomatitis virus from the nose. J. Neuropathol. Exp. Neurol. **47:**497–506.
19. **Luskin, M. B., and M. S. Boone.** 1994. Rate and pattern of migration of lineally-related olfactory bulb interneurons generated postnatally in the subventricular zone of the rat. Chem. Senses **19:**695–714.
20. **Mohammed, A. K. H., O. Magnusson, J. Maehen, F. Fonnum, E. Norrby, M. Schulzberg, and K. Kristensson.** 1990. Behavioural deficits and serotonin depletion in adult rats after transient infant nasal viral infection. Neuroscience **35:**355–363.
21. **Mohammed, A. K. H., J. Maehen, O. Magnusson, F. Fonnum, and K. Kristensson.** 1991. Persistent changes in behaviour and brain serotonin during aging in rats subjected to infant virus infection. Neurobiol. Aging **13:**83–87.
22. **Muller, U., U. Steinhoff, L. F. Reis, S. Hemmi, J. Pavlovic, R. M. Zinkerna-**

gel, and M. Aguet. 1994. Functional role of type I and type II interferons in antiviral defense. Science **264:**1918–1921.
23. **Plakhov, I. V., E. E. Arlund, C. Aoki, and C. S. Reiss.** 1995. The earliest events in vesicular stomatitis virus infection of the murine olfactory neuroepithelium and entry of the central nervous system. Virology **209:**257–262.
24. **Quiroz, E., N. Moreno, P. H. Peralta, and R. B. Tesh.** 1988. A human case of encephalitis associated with vesicular stomatitis virus (Indiana serotype) infection. Am. J. Trop. Med. Hyg. **39:**312–314.
25. **Reiss, C. S., I. V. Plakhov, and T. Komatsu.** 1998. Viral replication in olfactory receptor neurons and entry into the olfactory bulb and brain. Ann. N. Y. Acad. Sci. **855:**751–761.
26. **Roberts, A., and J. K. Rose.** 1999. Redesign and genetic dissection of the rhabdoviruses. Adv. Virus Res. **53:**301–319
27. **Roberts, A., E. Kretzschmar, A. S. Perkins, J. Forman, R. Price, L. Buonocore, Y. Kawaoka, and J. K. Rose.** 1998. Vaccination with a recombinant vesicular stomatitis virus expressing an influenza virus hemagglutinin provides complete protection from influenza virus challenge. J. Virol. **72:**4704–4711.
28. **Rodrigues, J. J., P. B. Singh, D. S. Dave, R. Prasan, V. Ayachit, B. H. Shaikh, and K. M. Pavri.** 1983. Isolation of Chandipura virus from the blood in acute encephalopathy syndrome. Ind. J. Med. Res. **77:**303–307.
29. **Rose, J. K., L. Buonocore, and M. A. Whitt.** 1991. A new cationic liposome reagent mediating nearly quantitative transfection of animal cells. BioTechniques **10:**520–525.
30. **Sabin, A. B., and P. K. Olitsky.** 1937. Influence of host factors on neuroinvasiveness of vesicular stomatitis virus. J. Exp. Med. **66:**15–34.
31. **Schlegel, R., T. S. Tralka, M. C. Willingham, and I. Patan.** 1983. Inhibition of VSV binding and infectivity by phosphatidylserine: is phosphatidylserine a VSV-binding site? Cell **32:**639–646.
32. **Schnell, M. J., L. Buonocore, E. Kretzschmar, E. Johnson, and J. K. Rose.** 1996. Foreign glycoproteins expressed from recombinant vesicular stomatitis viruses are incorporated efficiently into virus particles. Proc. Natl. Acad. Sci. USA **93:**11359–11365.
33. **Schnell, M. J., J. E. Johnson, L. Buonocore, and J. K. Rose.** 1997. Construction of a novel virus that targets HIV-1-infected cells and controls HIV-1 infection. Cell **90:**849–857.
34. **Shankar, V., M. Kao, A. N. Hamir, H. Sheng, H. Koprowski, and B. Dietzschold.** 1992. Kinetics of virus spread and changes in levels of several cytokine mRNAs in the brain after intranasal infection of rats with Borna disease virus. J. Virol. **66:**992–998
35. **Shepherd, G., and C. A. Greer.** 1990. Olfactory bulb, p. 133–169. *In* G. M. Shepherd (ed.), Synaptic organization of the brain. Oxford University Press, Oxford, United Kingdom.
36. **Smith, B. N., B. W. Banfield, C. A. Smeraski, C. L. Wilcox, F. E. Dudek, L. W. Enquist, and G. E. Pickard.** 2000. Pseudorabies virus expressing enhanced green fluorescent protein: a tool for in vitro electrophysiological analysis of transsynaptically labeled neurons in identified central nervous system circuits. Proc. Natl. Acad. Sci. USA **97:**9264–9269.
37. **Steinhoff, U., U. Müller, A. Schertler, H. Hengartner, M. Aguet, and R. M. Zinkernagel.** 1995. Antiviral protection by vesicular stomatitis virus-specific antibodies in alpha/beta interferon receptor-deficient mice. J. Virol. **69:**2153–2158.
38. **Stojdl, D. F., B. Lichty, S. Knowles, R. Marius, H. Atkins, N. Sonenberg, and J. C. Bell.** 2000. Exploiting tumor-specific defects in the interferon pathway with a previously unknown oncolytic virus. Nat. Med. **6:**821–825.
39. **Thomas, D., W. W. Newcomb, J. C. Brown, J. S. Wall, J. F. Hainfeld, B. L. Trus, and A. C. Steven.** 1985. Mass and molecular composition of vesicular stomatitis virus: a scanning transmission electron microscopy analysis. J. Virol. **54:**598–607.
40. **Tsukamoto, L. F., and R. W. Price.** 1982. Interferon protects neurons in culture infected with vesicular stomatitis and herpes simplex viruses. J. Neurol. Sci. **56:**115–128.
41. **van den Pol, A. N., E. Mocarski, N. Saederup, J. Vieira, and T. J. Meier.** 1999. Cytomegalovirus cell tropism, replication, and gene transfer in brain. J. Neurosci. **19:**10948–10965.
42. **Wagner, R. R., and J. K. Rose.** 1996. *Rhabdoviridae*: the viruses and their replication, p. 1121–1135. *In* B. N. Fields, D. M. Knipe, and P. M. Howley (ed.), Fields virology, 3rd ed. Lippincott-Raven, Philadelphia, Pa.
43. **Zemanick, M. C., P. L. Strick, and R. D. Dix.** 1991. Direction of transneuronal transport of herpes simplex virus 1 in the primate motor system is strain dependent. Proc. Natl. Acad. Sci. USA **88:**8048–8051.